

Itinerant Nature of Magnetism in Iron Pnictides: A first principles study

Yu-Zhong Zhang,¹ Ingo Opahle,¹ Harald O. Jeschke,¹ and Roser Valentí¹

¹*Institut für Theoretische Physik, Goethe-Universität Frankfurt,
Max-von-Laue-Straße 1, 60438 Frankfurt am Main, Germany*

(Dated: October 24, 2018)

Within the framework of density functional theory we investigate the nature of magnetism in various families of Fe-based superconductors. (i) We show that magnetization of stripe-type antiferromagnetic order always becomes stronger when As is substituted by Sb in LaOFeAs, BaFe₂As₂ and LiFeAs. By calculating Pauli susceptibilities, we attribute the magnetization increase obtained after replacing As by Sb to the enhancement of an instability at (π, π) . This points to a strong connection between Fermi surface nesting and magnetism, which supports the theory of the itinerant nature of magnetism in various families of Fe-based superconductors. (ii) We find that within the family LaOFePn ($Pn=P, As, Sb, Bi$) the absence of an antiferromagnetic phase in LaOFeP and its presence in LaOFeAs can be attributed to the competition of instabilities in the Pauli susceptibility at (π, π) and $(0, 0)$, which further strengthens the close relation between Fermi surface nesting and experimentally observed magnetization. (iii) Finally, based on our relaxed structures and Pauli susceptibility results, we predict that LaOFeSb upon doping or application of pressure should be a candidate for a superconductor with the highest transition temperature among the hypothetical compounds LaOFeSb, LaOFeBi, ScOFeP and ScOFeAs while the parent compounds LaOFeSb and LaOFeBi should show at ambient pressure a stripe-type antiferromagnetic metallic state.

PACS numbers: 74.70.-b 74.25.Ha 74.25.Jb,71.15.Mb,71.15.Pd

I. INTRODUCTION

After the discovery of the first high- T_c iron-based superconductor La[O_{1-x}F_x]FeAs¹ (denoted as 1111 compound), the superconducting transition temperature was rapidly raised up to 55 K with substitution of La by Sm². While various other families of Fe-based superconductors were reported afterwards, like the 122 compounds AFe_2As_2 ($A=Ca, Sr, Ba$)³⁻⁹, the 111 compounds $AFeAs$ ($A=Li, Na$)¹⁰⁻¹⁵ and the 11 compounds $FeCh$ ($Ch=Se, Te$)¹⁶⁻¹⁸, the transition temperature has always been lower than the highest one observed in the 1111 systems. Besides the continuous experimental attempts to pursue higher superconducting transition temperatures in the Fe-based compounds and deeper understanding of high- T_c superconductivity¹⁹, a great effort to understand the origin of their phase diagram has also been made on the theoretical side.

Although it is widely believed that magnetically mediated rather than phonon-mediated pairing dominates the superconducting state due to its proximity to a stripe-type antiferromagnetic phase²⁰⁻³⁷, the origin of the magnetism is still highly under debate. Some of the experimental work and theoretical studies based on density functional theory (DFT) support an itinerant scenario of magnetism due to the fact that the electron and hole sheets of the Fermi surface are nearly nested^{23,38-44} and correlation effects are not very strong, resulting in a metallic state of the parent compounds⁴⁵⁻⁴⁸. In contrast, some authors favor a localized picture^{21,34,35,49-53} since DFT calculations fail to reproduce the experimentally observed band splitting in the stripe-type antiferromagnetic phase⁵⁴. In these studies the observed small magnetic moment is attributed to highly frustrated su-

perexchange interactions which explain the observed low energy spin excitations well⁵⁵. Apart from the opposing viewpoints above, various other interpretations co-exist, such as those that propose that the magnetism could come from the local Hund's rule coupling⁵⁶ or from the coexistence of localized and itinerant electrons⁵⁷⁻⁶⁰. A recent LDA+U calculation explains the small magnetic moment by formation of magnetic multipoles⁶² while LDA+DMFT (dynamical mean field theory) calculations in conjunction with angle resolved photoemission (ARPES) experiments suggest that involvement of non-local fluctuations may be crucial⁶¹. Further, a recent DMFT calculation stressed the importance of the interplay between frustrated and unfrustrated bands within a two-band Hubbard model at half-filling⁶³. Among these theories, it is presently hard to decide which is the most promising for the observed magnetism in the parent compounds of the iron-based superconductors.

In fact, one of the most popular theories mentioned above, the itinerant scenario of magnetism, was recently substantially challenged both by experiment⁶⁴ and density functional theory calculations⁶⁵. On the one hand, an ARPES study on the 11 compound Fe_{1+x}Te shows no evidence of a Fermi surface nesting at $(\pi, 0)$ ⁶⁴ while magnetic order with such a wave vector is detected by neutron scattering⁶⁶. On the other hand, a DFT calculation on LaOFeAs, BaFe₂As₂ and LiFeAs based on a pseudopotential method⁶⁵ reveals that the magnetic moments are enhanced in all compounds by replacing As with Sb while the Fermi surface nesting with a nesting vector of (π, π) is found with this substitution to be enhanced only in the 1111 compound but suppressed in the 122 and 111 compounds. These studies question altogether the applicability of the theory of itinerant magnetism to the 11,

122 and 111 systems.

The former discrepancy in the 11 compounds was soon resolved by a new DFT calculation based on the full potential linear muffin tin orbital (FPLMTO) method which reconciles the theory of itinerant magnetism with the existing experiments on Fe_{1+x}Te ⁶⁷. It shows that, while the Fermi surface is nested at (π, π) in the undoped FeTe as in other iron-based superconductors, doping with 0.5 electrons due to the excess of Fe in Fe_{1+x}Te leads to a strong $(\pi, 0)$ nesting of the Fermi surface which corresponds to the observed magnetic ordering. However, up to now, the second question of enhanced Fermi surface nesting in 1111 versus suppression in 122 and 111 compounds when As is substituted by Sb still remains.

In this work, by applying Car-Parrinello molecular dynamics⁶⁸ based on a projector augmented wave (PAW) basis⁶⁹, we will show that, in contrast to the results from a pseudopotential method⁶⁵, the magnetic moment and the Pauli susceptibility at (π, π) are simultaneously enhanced when As is replaced by Sb in LaOFeAs , BaFe_2As_2 and LiFeAs , which strongly suggests that Fermi surface nesting is closely related to the magnetic moment strength, and the itinerant scenario of nesting-driven magnetism is still valid in the 111, 122 and 1111 compounds. By further comparing the Pauli susceptibilities of LaOFePn with $Pn=\text{P}$, As, Sb, and Bi, we argue that the absence and the presence of magnetism at ambient pressure in LaOFeP and LaOFeAs , respectively, originate from the competition between the instabilities of the susceptibility at $(0, 0)$ and (π, π) , which again indicates the importance of Fermi surface nesting for the description of magnetism. We predict that a stripe-type antiferromagnetic metallic state should be present in the hypothetical compounds LaOFeSb and LaOFeBi . Finally, we study the structural and magnetic properties of 1111 compounds including REOFeAs ($RE=\text{Ce}$, Nd, Sm), LaOFePn ($Pn=\text{P}$, As, Sb, Bi) and ScOFePn ($Pn=\text{P}$, As) and predict that LaOFeSb could be a superconductor with the highest transition temperature among these compounds.

II. METHOD

Throughout this paper, the Car-Parrinello⁶⁸ projector-augmented wave⁶⁹ method is employed to optimize the lattice parameters and internal atomic positions. These optimized structures are then used for all subsequent electronic structure calculations unless stated otherwise. $4 \times 4 \times 4$ \mathbf{k} -points and doubled ($\sqrt{2} \times \sqrt{2} \times 1$) unit cells with stripe-type antiferromagnetic order are used when relaxation of all lattice and electronic degrees of freedom is performed. We use time steps of 0.12 fs and friction to cool the systems to zero temperature. Note that the structure optimization is performed in the magnetic phase. As we shall show below, whenever experimental structures are available, our optimized structures compare well with the experimental ones. This is not the case

if structure optimizations are performed within non-spin polarized calculations as has been frequently pointed out in the literature.^{39,42,70}

We used high energy cutoffs of 408 eV and 1632 eV for the wave functions and charge density expansion, respectively. The total energy was converged to less than 0.01 meV/atom and the cell parameters to less than 0.0005 Å. Part of our results are double-checked by the full potential linearized augmented plane wave (FPLAPW) method as implemented in the WIEN2k code⁷¹ and full potential local orbital (FPLO) method⁷². Results are consistent among these methods. Throughout the paper, the Perdew-Burke-Ernzerhof generalized gradient approximation (GGA) to DFT has been used if not specified otherwise, and comparisons with the results from local density approximation (LDA) were also performed. In order to determine if the Fermi surface nesting is the driving force for the low-temperature stripe-type antiferromagnetic ordering, we calculate the \mathbf{q} -dependent Pauli susceptibility at $\omega=0$ and Fermi surface cuts at different k_z planes without magnetization. These calculations were performed with the WIEN2k code using $RK_{\text{max}} = 7$. While 40000 \mathbf{k} points in each k_z plane are used in calculating Fermi surface cuts, a three dimensional grid of $128 \times 128 \times 128$ \mathbf{k} and \mathbf{q} points and the constant matrix element approximation are employed for the susceptibility. For the calculations including Ce, Nd, and Sm atoms in the nonmagnetic phases, we apply the open core approximation for the localized f electrons. All calculations were performed in the scalar relativistic approximation, which usually provides a good description of structural properties even for heavier elements⁷³. Thus, spin-orbit coupling, which could be potentially relevant especially for Bi compounds^{74,75}, is neglected in the calculations for the valence electrons. However, since most of the weight of the Bi 6p states is well below the Fermi energy and irrelevant to magnetic ordering, we would expect only minor modifications for the resulting Fermi surfaces and susceptibilities.

III. PAULI SUSCEPTIBILITIES AND MAGNETISM IN 1111, 122 AND 111 COMPOUNDS

As is pointed out in Section I, a DFT calculation based on a pseudopotential method within the SIESTA code⁶⁵ reveals a disconnection between magnetism and Fermi surface nesting in 122 and 111 compounds, (*i.e.*, while magnetization is enhanced, the Pauli susceptibility at $\mathbf{q} = (\pi, \pi)$ which is responsible for stripe-type antiferromagnetic ordering is suppressed when As is replaced by Sb in BaFe_2As_2 and LiFeAs), and therefore questions the scenario of an itinerant nature of magnetism. From our spin-polarized GGA calculations for LaOFePn , BaFe_2Pn_2 and LiFePn ($Pn = \text{As}, \text{Sb}$), the same trends in magnetism are detected as observed in Ref. 65: the ground states are all found to be stripe-type antiferro-

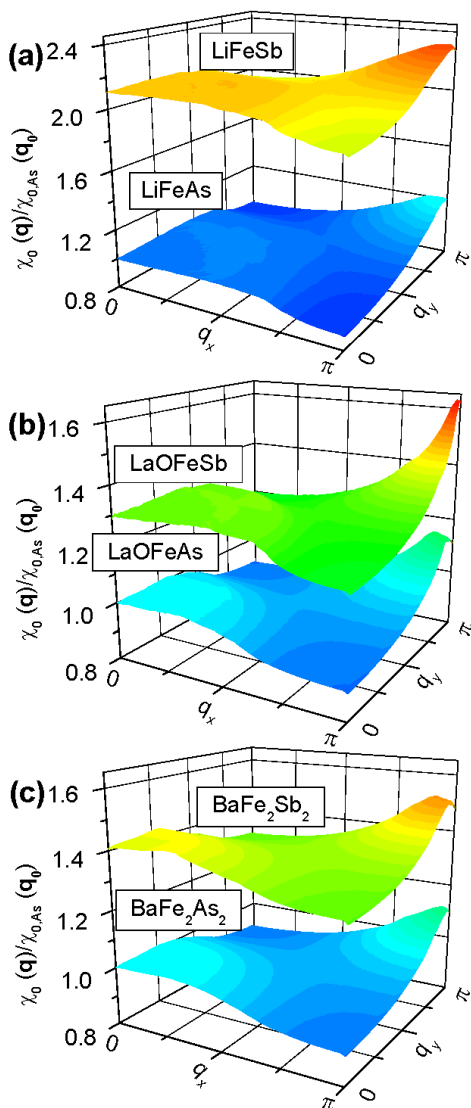


FIG. 1: (Color online) Comparison of normalized static \mathbf{q} -dependent Pauli susceptibilities at fixed $q_z = \pi$ between arsenide and antimonide of (a) 111 compounds, (b) 1111 compounds and (c) 122 compounds. The normalization factors are the susceptibilities of the corresponding arsenide systems for each type of compound at $\mathbf{q}_0 = (0, 0, \pi)$. Please note that the peak position is not exactly at $\mathbf{q}_\pi = (\pi, \pi, \pi)$ since the electron and hole Fermi surfaces are nearly nested rather than perfectly nested. Here, GGA is used for the DFT calculations.

magnetic metallic states and magnetic moments increase with the substitution of As by Sb in LaOFeAs, BaFe₂As₂ and LiFeAs.

However, the magnetic moments we obtained are 1.6 (2.3) μ_B in LiFeAs (LiFeSb), 2.0 (2.5) μ_B in BaFe₂As₂ (BaFe₂Sb₂) and 1.8 (2.2) μ_B in LaOFeAs (LaOFeSb)⁷⁶, which are notably smaller than those obtained from the pseudopotential method^{65,87}. Further comparing the optimized lattice structures, we find that, while our results are in good agreement with

TABLE I: Comparison between different DFT codes of the structures of LiFeAs optimized within GGA. $z_{Li}=0.3385$ and $z_{As}=0.7688$ are obtained from our CP-PAW calculations.

	$a(\text{\AA})$	$b(\text{\AA})$	$c(\text{\AA})$	$m(\mu_B)$	$d_{\text{Fe-As}}(\text{\AA})$
SIESTA ⁶⁵	5.482	5.285	6.190	2.54	2.434
VASP ⁸⁵	5.408	5.294	6.237	1.5	2.359
WIEN2k ⁸⁶	-	-	-	1.58	2.382
CP-PAW	5.422	5.307	6.255	1.56	2.385

previous GGA calculations, such as LiFeAs calculated with VASP⁸⁵ and WIEN2k⁸⁶, there are large differences between our results and those of Refs. 65,87 as shown in Table I. Furthermore, in Table II, we show the comparison between experimental and optimized structural data for BaFe₂As₂, where we find that our optimized structure agrees with the experimental one better than that from Ref. 65. Since the electronic band structure close to the Fermi level is sensitive to the lattice structure^{20,88}, the conclusion of Ref. 65 based on their optimized structures that there is no connection between Fermi surface nesting and magnetism is questionable. Therefore, we reinvestigate the nesting property of the Fermi surface.

TABLE II: Comparison between the experimental structure of BaFe₂As₂ and the optimized structures from different DFT codes within GGA. The magnetic moment on each Fe is also shown. $z_{As}=0.6495$ is obtained from our CP-PAW calculations.

	$a(\text{\AA})$	$b(\text{\AA})$	$c(\text{\AA})$	$m(\mu_B)$	$d_{\text{Fe-As}}(\text{\AA})$
Exp. ⁷⁸	5.616	5.571	12.943	0.87	2.392
SIESTA ⁶⁵	5.756	5.590	13.04	2.78	2.436
CP-PAW	5.693	5.666	13.008	1.98	2.396

Fig. 1 presents the comparison of normalized \mathbf{q} -dependent Pauli susceptibilities at fixed $q_z = \pi$ between arsenides and antimonides in 111, 1111 and 122 compounds. The normalization factors are the susceptibilities of the corresponding arsenide for each type of compounds at $\mathbf{q}_0 = (0, 0, \pi)$. We fix $q_z = \pi$ because of the fact that spins on iron are arranged antiferromagnetically along the z direction as observed in experiments⁷⁷⁻⁸¹. However, we checked that the conclusion drawn below will not be changed if $q_z = 0$ is fixed.

We find that in all Fe-based families, the situation is similar. Two peaks around $\mathbf{q}_0 = (0, 0, \pi)$ and $\mathbf{q}_\pi = (\pi, \pi, \pi)$ are detected in both arsenides and antimonides, and the peaks around (π, π, π) are always stronger than those around $(0, 0, \pi)$, indicating that the instability towards stripe-type antiferromagnetic ordering dominates, which is consistent with our spin-polarized GGA calculations. Most importantly, we find that, in contrast to Ref. 65, the Pauli susceptibilities are also enhanced together with the magnetizations when As is substituted by Sb in LaOFeAs, LiFeAs and BaFe₂As₂, which demon-

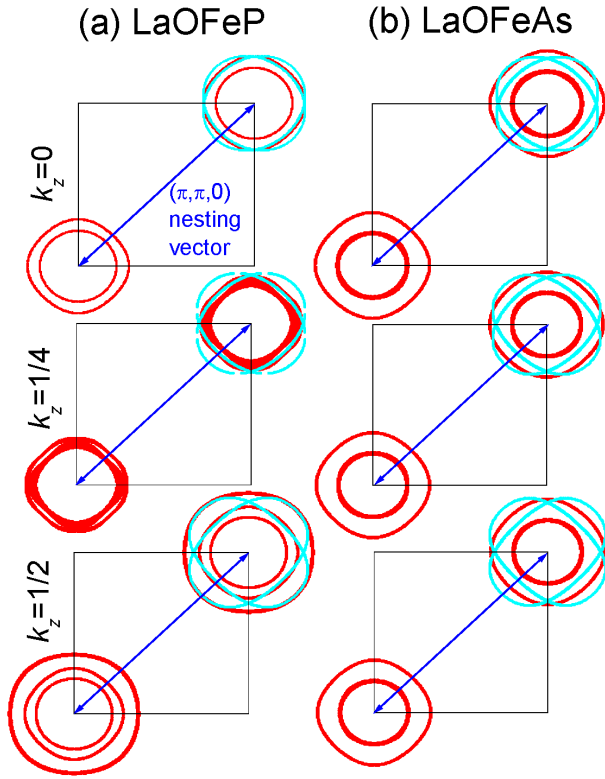


FIG. 2: (Color online) Fermi surface cuts for (a) LaOFeP and (b) LaOFeAs along different k_z -planes, where $k_z = n/4$, $n \in \{0, 1, 2\}$ in units of 2π . The cyan (light gray) curves are the electron Fermi surfaces around (π, π, k_z) and the red (dark gray) curves the hole Fermi surfaces around $(0, 0, k_z)$. In order to show the nesting properties, the hole Fermi surfaces at $(0, 0, k_z)$ are shown again, shifted by (π, π) . Here we use GGA for the DFT calculations.

strates a connection between Fermi surface nesting and magnetism and consequently strongly suggests that the theory of Fermi-surface-nesting-driven magnetism is still valid.

IV. COMPETITION OF INSTABILITIES IN PAULI SUSCEPTIBILITIES IN 1111 COMPOUNDS

TABLE III: Comparison of representative distances $d_{\text{Fe}-Pn}$ in (\AA) where $Pn=P, \text{As}, \text{Sb}$ and Bi in LaOFeP, LaOFeAs, LaOFeSb, and LaOFeBi between different GGA optimized structures and experimental structures, if available.

	Exp. ^{92,93}	CP-PAW	VASP ⁸⁹	SIESTA ⁶⁵
LaOFeP	2.289	2.264	2.232	-
LaOFeAs	2.408	2.372	2.357	2.446
LaOFeSb	-	2.547	2.50	2.660
LaOFeBi	-	2.639	-	-

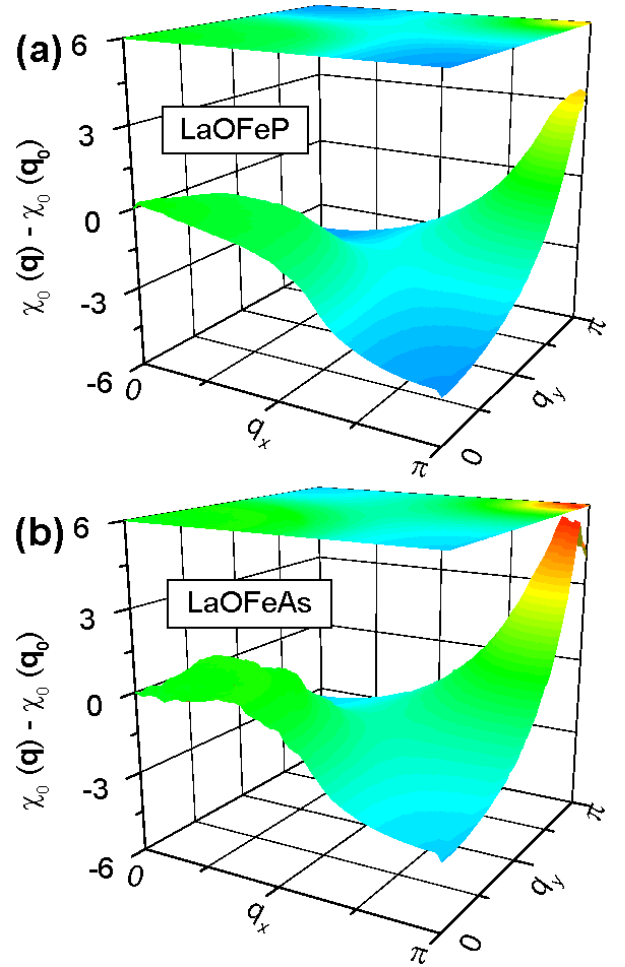


FIG. 3: (Color online) Static \mathbf{q} -dependent Pauli susceptibilities at fixed $q_z = \pi$ for (a) LaOFeP and (b) LaOFeAs. The corresponding values of the Pauli susceptibilities at $\mathbf{q}_0 = (0, 0, \pi)$ in LaOFeP and LaOFeAs, respectively, are subtracted. On top, two-dimensional contour maps are shown. Here, GGA is used for the DFT calculations.

TABLE IV: Comparison of representative distances $d_{\text{La}-\text{O}}$ in (\AA) in LaOFeP, LaOFeAs, LaOFeSb, and LaOFeBi between different GGA optimized structures and experimental structures, if available.

	Exp.	CP-PAW (ours)	VASP (ref.)	SIESTA ⁶⁵
LaOFeP	2.350	2.344	2.349	-
LaOFeAs	2.363	2.356	2.369	2.374
LaOFeSb	-	2.375	2.394	2.398
LaOFeBi	-	2.382	-	-

In what follows we concentrate on the 1111 compounds and perform a comparative study among LaOFePn ($Pn=P, \text{As}, \text{Sb}, \text{Bi}$). In Table III and IV, we first present the comparisons of two representative atomic distances among different structures optimized within GGA and experimental structures, if available. Our results agree

well with the experimental ones.

Fig. 2 shows the calculated Fermi surface cuts for LaOFeP and LaOFeAs on different k_z -planes based on the experimental lattice structures. The figure is almost unchanged if we consider the optimized lattice structure. The hole Fermi surfaces around $(0, 0, k_z)$ are shifted by $(\pi, \pi, 0)$ to show the nesting properties. Shifting of (π, π, π) was also investigated, and we find that the nesting properties are nearly unchanged. From the figure, it is apparent that the Fermi surface nesting is even more perfect in LaOFeP than in LaOFeAs, indicating a stronger tendency to stripe-type antiferromagnetic ordering in LaOFeP compared to LaOFeAs. However, experimentally, while a small magnetization is observed in undoped LaOFeAs⁷⁷, superconductivity rather than magnetic order is detected in undoped LaOFeP⁹⁰. These observations would indicate that Fermi surface nesting might not be connected to magnetization.

In order to quantify the Fermi surface nesting, we show in Fig. 3 the \mathbf{q} -dependent Pauli susceptibilities at fixed $q_z = \pi$ for LaOFeP and LaOFeAs with subtraction of the corresponding values at $\mathbf{q}_0 = (0, 0, \pi)$. While a peak in LaOFeP appears right at $\mathbf{q}_\pi = (\pi, \pi, \pi)$ indicating almost perfect nesting properties of the Fermi surfaces, peaks are situated close to $\mathbf{q}_\pi = (\pi, \pi, \pi)$ in LaOFeAs suggesting nearly nested Fermi surfaces, which is consistent with the Fermi surface cuts shown in Fig. 2. The most interesting finding in Fig. 3 is that the relative values $\chi(\pi, \pi, \pi) - \chi(0, 0, \pi)$ increase from LaOFeP to LaOFeAs irrespective of whether the Fermi surface nesting is perfect or not. While the peak at (π, π, π) favors stripe-type antiferromagnetic ordering, the one at $(0, 0, \pi)$ represents a possible instability towards checkerboard-type antiferromagnetic ordering or A-type antiferromagnetic ordering where ferromagnetic layers are stacked antiferromagnetically. The heights of these two peaks become closer in LaOFeP than in LaOFeAs, implying that competition between the above-mentioned two types of antiferromagnetic states becomes stronger in LaOFeP if thermal or quantum fluctuations are taken into account. Also spin-fluctuation mediated pairing of the superconducting state^{23,26,30} coming from inter-band scattering around $\mathbf{q}_\pi = (\pi, \pi, \pi)$ takes part in the competition. Eventually, as the two types of antiferromagnetism strongly compete with each other, the additional superconducting state order emerges and opens a gap, removing the high instability at the Fermi level and lowering the total energy. This could be the scenario to explain why undoped LaOFeP is always nonmagnetic but shows superconductivity below 3.2 K at ambient pressure. As $\chi(\pi, \pi, \pi) - \chi(0, 0, \pi)$ increases beyond a critical value, the stripe-type antiferromagnetic ordering prevails over the checkerboard-type one and the pairing. This scenario may apply to the low-temperature magnetic phase of LaOFeAs. Furthermore, we have calculated the total energies of checkerboard and stripe-type antiferromagnetic phases for both LaOFeP and LaOFeAs. We found that the stripe-type antiferromagnetic phases are the ground state in both

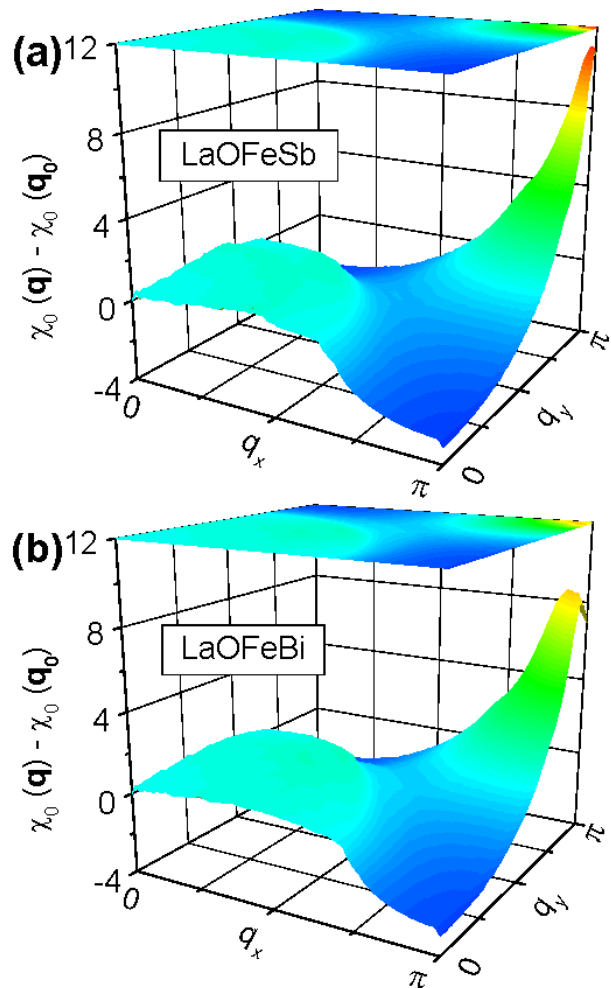


FIG. 4: (Color online) Static \mathbf{q} -dependent Pauli susceptibilities at fixed $q_z = \pi$ for (a) LaOFeSb and (b) LaOFeBi. The corresponding values of the Pauli susceptibilities at $\mathbf{q}_0 = (0, 0, \pi)$ in LaOFeSb and LaOFeBi, respectively, are subtracted. On top, two-dimensional contour maps are shown. In the DFT calculations GGA is used.

cases and the energy difference between the two phases is smaller in LaOFeP than in LaOFeAs, which is consistent with the trend of $\chi(\pi, \pi, \pi) - \chi(0, 0, \pi)$.

In Fig. 4, we display the \mathbf{q} -dependent Pauli susceptibilities at fixed $q_z = \pi$ for the hypothetical compounds LaOFeSb and LaOFeBi. The corresponding values of the Pauli susceptibilities at $\mathbf{q}_0 = (0, 0, \pi)$ in LaOFeSb and LaOFeBi, respectively, are again subtracted. Note that $\chi(\pi, \pi, \pi) - \chi(0, 0, \pi)$ in LaOFeSb and LaOFeBi is even larger than that in LaOFeAs (see Fig. 3), indicating that the instability towards stripe-type antiferromagnetic ordering could win the competition between different instabilities in these two compounds. It is also interesting to note that the peak at $\mathbf{q}_0 = (0, 0, \pi)$ becomes flatter when we go from LaOFeP to LaOFeBi. While the flatness of the peak can be associated with a larger number of different magnetic structures lying

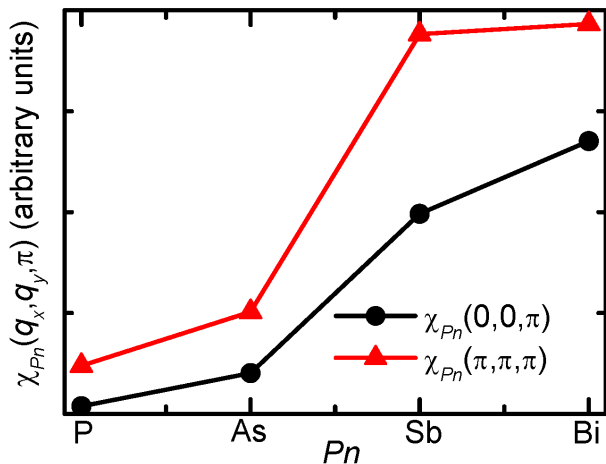


FIG. 5: (Color online) Static Pauli susceptibilities at $\mathbf{q}_0 = (0, 0, \pi)$ and $\mathbf{q}_\pi = (\pi, \pi, \pi)$ for $\text{LaOFe}Pn$ with $Pn=\text{P, As, Sb, Bi}$. Here we use GGA for the DFT calculations.

within a small energy window, the stronger peaks around $\mathbf{q}_\pi = (\pi, \pi, \pi)$ compared to $\mathbf{q}_0 = (0, 0, \pi)$ in all the 1111 compounds we studied makes other magnetic orderings besides the stripe-type antiferromagnetic one less favorable. Combining the results from spin-polarized GGA (LSDA) calculations where magnetic moments on each iron are given as 2.2 (1.3) and 2.4 (1.8) μ_B in LaOFeSb and LaOFeBi , respectively, we predict that the ground states of these two compounds at ambient pressure without doping should show stripe-type antiferromagnetic order although spin-polarized GGA (LSDA) calculations overestimate the magnetic moments.

The increase of the magnetic moment from As to Sb to Bi can be understood from Fig. 5 where Pauli susceptibilities at $\mathbf{q}_0 = (0, 0, \pi)$ and $\mathbf{q}_\pi = (\pi, \pi, \pi)$ for $\text{LaOFe}Pn$ with $Pn=\text{P, As, Sb, Bi}$ are explicitly shown. While the increasing absolute value of $\chi_{Pn}(\pi, \pi, \pi)$ as Pn changes from P to Bi is probably responsible for the increasing magnetic moment, the difference between $\chi_{Pn}(\pi, \pi, \pi)$ and $\chi_{Pn}(0, 0, \pi)$ dominates the possible competition between different ordered states, which again implies a strong relation between Fermi surface nesting and magnetism. Due to the fact that LaOFeAs is not a superconductor without doping or application of pressure, we argue that possible superconducting states in LaOFeSb and LaOFeBi can only occur under doping or application of pressure.

In Fig. 6, we display the DOS for LaOFeAs , LaOFeSb and LaOFeBi calculated within spin-polarized GGA calculations. It is shown that in all three cases the DOS at the Fermi level remains finite, suggesting that undoped LaOFeSb and LaOFeBi are stripe-type antiferromagnetic metals at ambient pressure as is the case of LaOFeAs or other iron-based superconductors. Our results from spin-polarized GGA calculations cannot corroborate the arguments introduced in Ref. 91 where it is argued that LaOFeSb and LaOFeBi could be antiferromagnetic Mott insulators, though the tendency towards larger Fe mag-

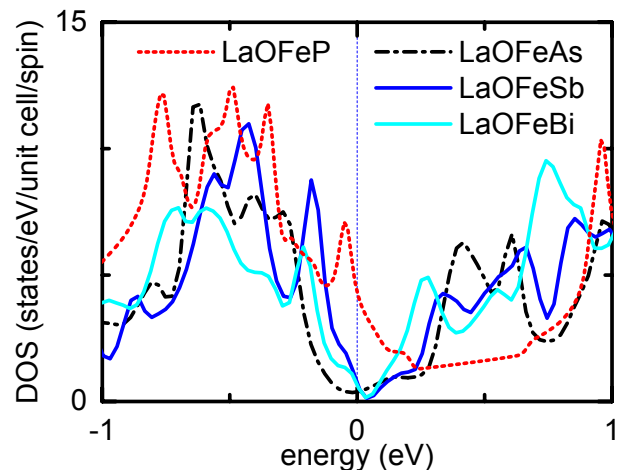


FIG. 6: (Color online) Total density of states (DOS) for LaOFeAs , LaOFeSb and LaOFeBi in the low-temperature orthorhombic phase with stripe-type antiferromagnetic order calculated by spin-polarized GGA. Also shown for comparison is the DOS for nonmagnetic LaOFeP calculated by GGA. Relatively high DOS at the Fermi level is present in LaOFeP , indicating the possible instability with respect to superconductivity in the absence of magnetic order.

netic moments from the As to Bi compounds is observed. Such a conclusion is also confirmed by our LSDA calculations. In Fig. 6, the DOS for LaOFeP is also shown. Since LaOFeP is nonmagnetic at low temperature, only the non-spinpolarized GGA result is presented. It is found that the DOS at the Fermi level remains relatively high, which indicates a possible instability with respect to superconductivity in the absence of magnetic order with the opening of a superconducting gap and the lifting of the degeneracy at the Fermi level.

V. NEW SUPERCONDUCTOR CANDIDATES

Experimentally, the highest recorded superconducting transition temperature has been observed in the 1111 compounds. It is therefore tempting to find ways to predict T_c for hypothetical 1111 compounds. One promising route is to consider a phenomenological relation between T_c and the $\chi(\pi, \pi, \pi) - \chi(0, 0, \pi)$ of the parent compound. As we know, with doping or application of pressure, the $\chi(\pi, \pi, \pi)$ instability is suppressed, resulting in the disappearance of stripe-type antiferromagnetic order. However, strong inter-band scattering with a wave vector around (π, π, π) compared to intra-band scattering with a wave vector around $(0, 0, \pi)$ remains, which leads to a superconducting state. Therefore we argue that the larger the relative value of $\chi(\pi, \pi, \pi) - \chi(0, 0, \pi)$ in the parent compound is, the stronger the antiferromagnetic spin fluctuation after suppression of magnetic order, and thus the higher the superconducting transition temperature will be.

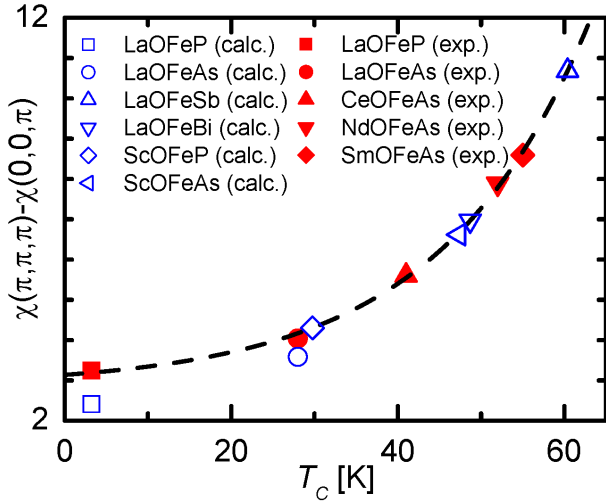


FIG. 7: (Color online) Prediction of superconducting transition temperatures T_c from a phenomenological relation between T_c and $\chi(\pi, \pi, \pi) - \chi(0, 0, \pi)$ for the parent compounds of the hypothetical 1111 compounds LaOFeSb, LaOFeBi, ScOFeP and ScOFeAs. The phenomenological relation was determined by calculating $\chi(\pi, \pi, \pi) - \chi(0, 0, \pi)$ for several 1111 compounds LaOFeP, LaOFeAs, CeOFeAs, NdOFeAs, and SmOFeAs by GGA where T_c 's and lattice structures are given experimentally. The $\chi(\pi, \pi, \pi) - \chi(0, 0, \pi)$ for LaOFeP and LaOFeAs calculated by GGA from DFT optimized structures are also shown for comparison. It is found that the resulting $\chi(\pi, \pi, \pi) - \chi(0, 0, \pi)$ for LaOFeP and LaOFeAs based on our optimized structures is only slightly underestimated compared to that calculated from experimental structures, which shows that the result depends only weakly on our structure optimization.

In Fig. 7, we plot $\chi(\pi, \pi, \pi) - \chi(0, 0, \pi)$ versus T_c for the hypothetical 1111 compounds LaOFeSb, LaOFeBi, ScOFeP and ScOFeAs. The phenomenological relation between T_c and $\chi(\pi, \pi, \pi) - \chi(0, 0, \pi)$ is determined by first calculating $\chi(\pi, \pi, \pi) - \chi(0, 0, \pi)$ for several typical 1111 compounds LaOFeP^{90,92}, LaOFeAs^{1,93}, CeOFeAs^{94,95}, NdOFeAs^{96,97}, and SmOFeAs^{98,99}, where T_c and lattice structures are given experimentally, and then fitting the data by an exponential growth function of $\chi(\pi, \pi, \pi) - \chi(0, 0, \pi) = 2.86 + 0.28 * \exp(T_c/18.14)$. With this relation, T_c for the compounds which have not yet been experimentally reported is predicted by optimizing the lattice structure and calculating $\chi(\pi, \pi, \pi) - \chi(0, 0, \pi)$ from DFT calculations. From Fig. 7, we find that the resulting $\chi(\pi, \pi, \pi) - \chi(0, 0, \pi)$ for LaOFeP and LaOFeAs based on our optimized structures is only slightly underestimated compared to that calculated from experimental structures, which shows that the result depends only weakly on our structure optimization. Among the four 1111 compounds, this procedure shows that LaOFeSb can give the highest T_c around 60 K which is above the highest recorded T_c of 55 K in SmOFeAs.

An alternative procedure to predict T_c phenomenologically is based on the fact that the physical properties

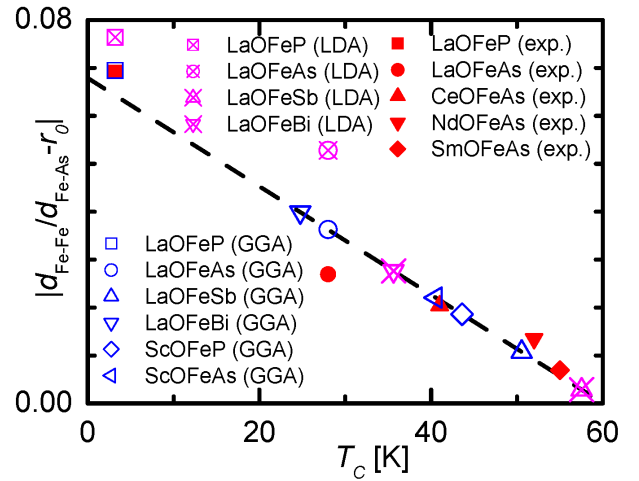


FIG. 8: (Color online) Prediction of superconducting transition temperatures T_c from a phenomenological relation between T_c and the ratio of atomic distances $d_{\text{Fe-Fe}}$ and $d_{\text{Fe-As}}$ for the hypothetical 1111 compounds LaOFeSb, LaOFeBi, ScOFeP and ScOFeAs. A constant ratio of $r_0 = d_{0,\text{Fe-Fe}}/d_{0,\text{Fe-As}}$ for distances $d_{0,\text{Fe-Fe}}$, $d_{0,\text{Fe-As}}$ in a perfect FeAs_4 tetrahedron is subtracted. The phenomenological relation is determined by taking into account the same compounds LaOFeP, LaOFeAs, CeOFeAs, NdOFeAs, and SmOFeAs as in Fig. 7 where T_c and lattice structures are given experimentally and doing a linear fit as in Ref. 95. The $|d_{\text{Fe-Fe}}/d_{\text{Fe-As}} - r_0|$ for LaOFeP, LaOFeAs, LaOFeSb, and LaOFeBi based on optimized structures within GGA and LDA are also shown for comparisons. Comparing the results for LaOFeP and LaOFeAs from GGA and LDA optimizations with those from experiments, we find that the optimized structures from GGA are more consistent with the experimental one.

of Fe-based superconductors strongly depend on the As position. Tiny shiftings of the As position away from or closer to the iron plane will significantly change the band structure around the Fermi level^{20,88}. Therefore, similar to Refs. 95 and 100, we plot in Fig. 8 T_c versus the absolute value of the ratio between atomic distances $d_{\text{Fe-Fe}}$ and $d_{\text{Fe-As}}$ while subtracting $r_0 = d_{0,\text{Fe-Fe}}/d_{0,\text{Fe-As}}$ where $d_{0,\text{Fe-Fe}}$ and $d_{0,\text{Fe-As}}$ denote the distances in a perfect tetrahedron formed by four nearest neighbor As atoms surrounding one Fe atom. Similar to the first scheme, we determine the phenomenological relation between $|d_{\text{Fe-Fe}}/d_{\text{Fe-As}} - r_0|$ and T_c by taking into account the same compounds LaOFeP, LaOFeAs, CeOFeAs, NdOFeAs, and SmOFeAs as in the first scheme where T_c and lattice structures are given experimentally and doing a linear fit as in Ref. 95. With this relation, the T_c for LaOFeSb, LaOFeBi, ScOFeP and ScOFeAs is predicted based on the optimized structure.

Fig. 8 presents the results based on the structures optimized within both GGA and LDA. Comparing the results for LaOFeP and LaOFeAs from GGA and LDA optimizations with those from experiments, we find that the optimized structures from GGA are more consis-

tent with the experimental one. According to the relation we fitted, LaOFeSb always gives the highest T_c of 57.5 (50.6) K for LDA (GGA) optimizations, respectively, among the four 1111 compounds we studied. Combining the two presented phenomenological prediction schemes, we clearly obtain that LaOFeSb would be upon doping or under pressure a good candidate for superconductivity with highest T_c and it would be very interesting to see it synthesized.

VI. CONCLUSIONS

In the present work we studied the physical properties of LaOFePn, BaFe₂Pn₂ and LiFePn with Pn=As and Sb. Our results support the validity of the itinerant nature of magnetism in these compounds where magnetization is closely related to Fermi surface nesting. Furthermore, we concentrated on the 1111 compounds LaOFePn with Pn=P, As, Sb, and Bi. We found that the increase of the magnetic moment in the undoped compounds with Pn varying from P to Bi is due to the increasing instability of the Pauli susceptibility at $\mathbf{q}_\pi = (\pi, \pi, \pi)$ and the decreasing competition to the instability at $\mathbf{q}_0 = (0, 0, \pi)$. The superconducting state appearing in undoped LaOFeP at ambient pressure is ascribed to the strong competition between the instability at $\mathbf{q}_\pi = (\pi, \pi, \pi)$ and $\mathbf{q}_0 = (0, 0, \pi)$. Thus, together with the investigation of the DOS in the

low temperature phase, we argue that the hypothetical compounds LaOFeSb and LaOFeBi are antiferromagnetic metals at ambient pressure without doping. The results for LaOFePn again strongly imply that Fermi surface nesting plays a dominating role in the physical properties of the 1111 compounds. Finally we consider two phenomenological relations to predict the superconducting transition temperature T_c for the hypothetical 1111 compounds and predict that LaOFeSb would be a possible candidate for a superconductor with a higher T_c than presently recorded for the known Fe-based superconductors. Combining the fact that Fermi surface nesting dominates the physics in the 122 compounds, 1111 compounds, 11 compounds, and 111 compounds, we argue that magnetism in iron-based superconductors is strongly influenced by their itinerant nature. However, from our study, the localized scenario is not ruled out and may also play an important role in the physics of iron-based superconductors. Furthermore, while in our study we emphasize the role of the states at the Fermi level and accordingly the nesting property of the Fermi surface on the itinerant nature of magnetism, the significant contributions to the finite moment of itinerant magnetism from the states in the vicinity of the Fermi level should not be ignored.

Acknowledgments.- We would like to thank the Deutsche Forschungsgemeinschaft for financial support through the SFB/TRR 49 and Emmy Noether programs.

-
- ¹ Y. Kamihara, T. Watanabe, M. Hirano, and H. Hosono, *J. Am. Chem. Soc.* **130**, 3296 (2008).
- ² Z. A. Ren, W. Lu, J. Yang, W. Yi, X. L. Shen, Z. C. Li, G. C. Che, X. L. Dong, L. L. Sun, F. Zhou, and Z. X. Zhao, *Chin. Phys. Lett.* **25**, 2215 (2008).
- ³ Milton S. Torikachvili, Sergey L. Bud'ko, Ni Ni, and Paul C. Canfield, *Phys. Rev. Lett.* **101**, 057006 (2008).
- ⁴ K. Sasmal, B. Lv, B. Lorenz, A. M. Guloy, F. Chen, Y. Xue and P. C. W. Chu, *Phys. Rev. Lett.* **101**, 107007 (2008).
- ⁵ G. F. Chen, Z. Li, G. Li, Z. Hu, J. Dong, X. D. Zhang, P. Zheng, N. L. Wang and J. L. Luo, *Chin. Phys. Lett.* **25**, 3403 (2008).
- ⁶ M. Rotter, M. Tegel and D. Johrendt, *Phys. Rev. Lett.* **101**, 107006 (2008).
- ⁷ P. L. Alireza, Y. T. C. Ko, J. Gillett, C. M. Petrone, J. M. Cole, G. G. Lonzarich and S. E. Sebastian, *J. Phys.: Condens. Matter* **21**, 012208 (2009).
- ⁸ S. A. J. Kimber, A. Kreyssig, Y.-Z. Zhang, H. O. Jeschke, R. Valentí, F. Yokaichiya, E. Colombier, J. Yan, T. C. Hansen, T. Chatterji, R. J. McQueeney, P. C. Canfield, A. I. Goldman and D. N. Argyriou, *Nature Materials* **8**, 471 (2009).
- ⁹ A. S. Sefat, R. Jin, M. A. McGuire, B. C. Sales, D. J. Singh, and D. Mandrus, *Phys. Rev. Lett.* **101**, 117004 (2008).
- ¹⁰ X. C. Wang, Q. Liu, Y. Lv, W. Gao, L. X. Yang, R. C. Yu, F. Y. Li, and C. Jin, *Solid. State. Commun.* **148**, 538 (2008).
- ¹¹ J. H. Tapp, Z. Tang, B. Lv, K. Sasmal, B. Lorenz, P. C. W. Chu, and A. M. Guloy, *Phys. Rev. B* **78**, 060505 (2008).
- ¹² M. J. Pitcher, D. R. Parker, P. Adamson, S. J. C. Herkelrath, A. T. Boothroyd, R. M. Ibberson, M. Brunelli, and S. J. Clarke, *Chem. Commun.* **2008**, 5918 (2008).
- ¹³ S. J. Zhang, X. C. Wang, R. Sammynaiken, J. S. Tse, L. X. Yang, Z. Li, Q. Q. Liu, S. Desgreniers, Y. Yao, H. Z. Liu, and C. Q. Jin, *Phys. Rev. B* **80**, 014506 (2009).
- ¹⁴ D. R. Parker, M. J. Pitcher, P. J. Baker, I. Franke, T. Lancaster, S. J. Blundell, and S. J. Clarke, *Chem. Commun. (Cambridge)* **(2009)**, 2189.
- ¹⁵ G. F. Chen, W. Z. Hu, J. L. Luo, and N. L. Wang, *Phys. Rev. Lett.* **102**, 227004 (2009).
- ¹⁶ F.-C. Hsu, J.-Y. Luo, K.-W. Yeh, T.-K. Chen, T.-W. Huang, P. M. Wu, Y.-C. Lee, Y.-L. Huang, Y.-Y. Chu, D.-C. Yan, and M.-K. Wu, *Proc. Natl. Acad. Sci. U.S.A.* **105**, 14262 (2008).
- ¹⁷ Y. Mizuguchi, F. Tomioka, S. Tsuda, T. Yamaguchi, and Y. Takano, *Appl. Phys. Lett.* **93**, 152505 (2008).
- ¹⁸ K.-W. Yeh, T.-W. Huang, Y. Lin Huang, T.-K. Chen, F.-C. Hsu, P. M. Wu, Y.-C. Lee, Y.-Y. Chu, C.-L. Chen, J.-Y. Luo, D.-C. Yan, and M.-K. Wu, *Europhys. Lett.* **84** 37002 (2008).
- ¹⁹ H. Q. Yuan, J. Singleton, F. F. Balakirev, S. A. Baily, G. F. Chen, J. L. Luo, N. L. Wang, *Nature* **457**, 565 (2009).
- ²⁰ D. J. Singh and M.-H. Du, *Phys. Rev. Lett.* **100**, 237003 (2008).

- (2008).
- 21 K. Haule, J. H. Shim, and G. Kotliar, Phys. Rev. Lett. **100**, 226402 (2008).
 - 22 L. Boeri, O. V. Dolgov, and A. A. Golubov, Phys. Rev. Lett. **101**, 026403 (2008).
 - 23 I. I. Mazin, D. J. Singh, M. D. Johannes and M. H. Du, Phys. Rev. Lett. **101**, 057003 (2008).
 - 24 I. I. Mazin, J. Schmalian, Physica C **469**, 614 (2009).
 - 25 F. Wang, H. Zhai, and D. Lee, Europhys. Lett. **85**, 37005 (2009).
 - 26 A. V. Chubukov, D. Efremov, and I. Eremin, Phys. Rev. B **78**, 134512 (2008).
 - 27 V. Stanev, J. Kang, and Z. Tesanovic, Phys. Rev. B **78**, 184509 (2008).
 - 28 K. Kuroki, S. Onari, R. Arita, H. Usui, Y. Tanaka, H. Kontani, and H. Aoki, Phys. Rev. Lett. **101**, 087004 (2008).
 - 29 S. Graser, G. R. Boyd, C. Cao, H.-P. Cheng, P. J. Hirschfeld, and D. J. Scalapino, Phys. Rev. B **77**, 180514(R) (2008).
 - 30 S. Graser, T. A. Maier, P. J. Hirschfeld, D. J. Scalapino, New J. Phys. **11**, 025016 (2009).
 - 31 X.-L. Qi, S. Raghu, C.-X. Liu, D. J. Scalapino, and S.-C. Zhang, arXiv:0804.4332 (unpublished).
 - 32 Z.-J. Yao, J.-X. Li, and Z. D. Wang, New J. Phys. **11**, 025009 (2009).
 - 33 R. Sknepnek, G. Samolyuk, Y. Lee, J. Schmalian, Phys. Rev. B **79**, 054511 (2009).
 - 34 Q. Si and E. Abrahams, Phys. Rev. Lett. **101**, 076401 (2008).
 - 35 T. Yildirim, Phys. Rev. Lett. **101**, 057010 (2008).
 - 36 K. Seo, B. A. Bernevig, and J. Hu, Phys. Rev. Lett. **101**, 206404 (2008).
 - 37 K. Ishida, Y. Nakai, H. Hosono, J. Phys. Soc. Jpn. **78**, 062001 (2009).
 - 38 D. Hsieh, Y. Xia, L. Wray, D. Qian, K. Gomes, A. Yazdani, G. F. Chen, J. L. Luo, N. L. Wang, M. Z. Hasan, arXiv:0812.2289 (unpublished).
 - 39 J. Fink, S. Thirupathiah, R. Ovsyannikov, H. A. Dürr, R. Follath, Y. Huang, S. de Jong, M. S. Golden, Yu-Zhong Zhang, H. O. Jeschke, R. Valentí, C. Felser, S. Dastjani Farahani, M. Rotter, and D. Johrendt, Phys. Rev. B **79**, 155118 (2009).
 - 40 V. Cvetkovic and Z. Tesanovic, Europhys. Lett. **85**, 37002 (2009).
 - 41 J. Dong, H. J. Zhang, G. Xu, Z. Li, G. Li, W. Z. Hu, D. Wu, G. F. Chen, X. Dai, J. L. Luo, Z. Fang, and N. L. Wang, Europhys. Lett. **83**, 27006 (2008).
 - 42 I. Opahle, H. C. Kandpal, Y. Zhang, C. Gros, and R. Valentí, Phys. Rev. B **79**, 024509 (2009).
 - 43 Y.-Z. Zhang, H. C. Kandpal, I. Opahle, H. O. Jeschke, and R. Valentí, Phys. Rev. B **80**, 094530 (2009).
 - 44 A. N. Yaresko, G.-Q. Liu, V. N. Antonov, O.K. Andersen, Phys. Rev. B **79**, 144421 (2009).
 - 45 T. Kroll, S. Bonhommeau, T. Kachel, H. A. Dürr, J. Werner, G. Behr, A. Koitzsch, R. Hübel, S. Leger, R. Schönfelder, A. K. Ariffin, R. Mancke, F. M. F. de Groot, J. Fink, H. Eschrig, B. Büchner, and M. Knupfer, Phys. Rev. B **78**, 220502(R) (2008).
 - 46 S. L. Skornyakov, A. V. Efremov, N. A. Skorikov, M. A. Korotin, Yu. A. Izyumov, V. I. Anisimov, A. V. Kozhevnikov, and D. Vollhardt, Phys. Rev. B **80**, 092501 (2009).
 - 47 W. L. Yang, A. P. Sorini, C.-C. Chen, B. Moritz, W.-S. Lee, F. Vernay, P. Olalde-Velasco, J. D. Denlinger, B. Delley, J.-H. Chu, J. G. Analytis, I. R. Fisher, Z. A. Ren, J. Yang, W. Lu, Z. X. Zhao, J. van den Brink, Z. Hussain, Z.-X. Shen, and T. P. Devereaux, Phys. Rev. B **80**, 014508 (2009).
 - 48 M. Aichhorn, L. Pourovskii, V. Vildosola, M. Ferrero, O. Parcollet, T. Miyake, A. Georges, and S. Biermann, Phys. Rev. B **80**, 085101 (2009).
 - 49 M. J. Han, Q. Yin, W. E. Pickett, and S. Y. Savrasov, Phys. Rev. Lett. **102**, 107003 (2009).
 - 50 L. Craco, M. S. Laad, S. Leoni, and H. Rosner, Phys. Rev. B **78**, 134511 (2008).
 - 51 F. Ma, Z.-Y. Lu, T. Xiang, Phys. Rev. B **78**, 224517 (2008).
 - 52 F. Ma, W. Ji, J. Hu, Z.-Y. Lu, T. Xiang, Phys. Rev. Lett. **102**, 177003 (2009).
 - 53 F. Krüger, S. Kumar, J. Zaanen, and J. van den Brink, Phys. Rev. B **79**, 054504 (2009).
 - 54 L. Yang Y. Zhang, H. Ou, J. Zhao, D. Shen, B. Zhou, J. Wei, F. Chen, M. Xu, C. He, Y. Chen, Z. Wang, X. Wang, T. Wu, G. Wu, X. Chen, M. Arita, K. Shimada, M. Taniguchi, Z. Lu, T. Xiang, and D. Feng, Phys. Rev. Lett. **102**, 107002 (2009).
 - 55 B. Schmidt, M. Siahatgar, P. Thalmeier, arXiv:0911.5664 (unpublished).
 - 56 M. D. Johannes and I. I. Mazin, Phys. Rev. B **79**, 220510(R) (2009).
 - 57 J. Wu, P. Phillips, and A. H. Castro Neto, Phys. Rev. Lett. **101**, 126401 (2008).
 - 58 J. Wu and P. Phillips, arXiv:0901.3538 (unpublished).
 - 59 S.-P. Kou, T. Li, and Z.-Y. Weng, arXiv:0811.4111 (unpublished).
 - 60 F. Wang, H. Zhai and D.-H. Lee, Europhys. Lett. **85**, 37005 (2009).
 - 61 J. Sanchez-Barriga, J. Fink, V. Boni, I. Di Marco, J. Braun, J. Minar, A. Varykhalov, O. Rader, V. Bellini, F. Manghi, H. Ebert, M. I. Katsnelson, A. I. Lichtenstein, O. Eriksson, W. Eberhardt, H. A. Dürr, Phys. Rev. Lett. **103**, 267203 (2009).
 - 62 F. Cricchio, O. Grånäs, L. Nordström, arXiv:0911.1342 (unpublished).
 - 63 H. Lee, Y.-Z. Zhang, H. O. Jeschke, and R. Valentí, arXiv:0912.4024 (unpublished).
 - 64 Y. Xia, D. Qian, L. Wray, D. Hsieh, G. F. Chen, J. L. Luo, N. L. Wang, and M. Z. Hasan, Phys. Rev. Lett. **103**, 037002 (2009).
 - 65 C.-Y. Moon, S. Y. Park, and H. J. Choi, Phys. Rev. B **80**, 054522 (2009).
 - 66 S. Li, C. de la Cruz, Q. Huang, Y. Chen, J. W. Lynn, J. Hu, Y.-L. Huang, F.-C. Hsu, K.-W. Yeh, M.-K. Wu, and P. Dai, Phys. Rev. B **79**, 054503 (2009).
 - 67 M. J. Han and S. Y. Savrasov, Phys. Rev. Lett. **103**, 067001 (2009).
 - 68 R. Car, M. Parrinello, Phys. Rev. Lett. **55**, 2471 (1985).
 - 69 P. E. Blöchl, Phys. Rev. B **50**, 17953 (1994).
 - 70 I. I. Mazin, M. D. Johannes, L. Boeri, K. Koepnik, and D. J. Singh, Phys. Rev. B **78**, 085104 (2008).
 - 71 P. Blaha, K. Schwarz, G. Madsen, D. Kvaniscka, and J. Luitz, WIEN2K, An Augmented Plane Wave+Local Orbitals Program for Calculating Crystal, edited by K. Schwarz (Techn. University, Vienna, Austria, 2001).
 - 72 K. Koepnik and H. Eschrig, Phys. Rev. B **59**, 1743 (1999). <http://www.FPLO.de>
 - 73 H. Eschrig, M. Richter, and I. Opahle, in: *Relativistic*

- Electronic Structure Theory - Part II: Applications*, Ed. P. Schwerdtfeger (Elsevier, Amsterdam 2004), pp. 723–776.
- ⁷⁴ N. Kozlova, J. Hagel, M. Doerr, J. Wosnitza, D. Eckert, K.-H. Müller, L. Schultz, I. Opahle, S. Elgazzar, Manuel Richter, G. Goll, H. v. Löhneysen, G. Zwicknagl, T. Yoshino, T. Takabatake, *Phys. Rev. Lett.* **95**, 086403 (2005).
- ⁷⁵ J. Wosnitza, G. Goll, A. D. Bianchi, B. Bergk, N. Kozlova, I. Opahle, S. Elgazzar, Manuel Richter, O. Stockert, H. v. Löhneysen, T. Yoshino, and T. Takabatake, *New J. Phys.* **8**, 174 (2006).
- ⁷⁶ It is well-known that the magnetic moments are overestimated by GGA^{42,43,70} when compared to experimental data^{13,77–81} or even to LDA calculations^{42,82–84}. The reason for choosing GGA for the structure optimization is that the GGA optimized structures are more consistent with experiment than the LDA ones^{43,70}.
- ⁷⁷ Clarina de la Cruz, Q. Huang, J. W. Lynn, Jiying Li, W. Ratcliff II, J. L. Zarestky, H. A. Mook, G. F. Chen, J. L. Luo, N. L. Wang, and Pengcheng Dai, *Nature* **453**, 899 (2008).
- ⁷⁸ Q. Huang, Y. Qiu, Wei Bao, M. A. Green, J. W. Lynn, Y. C. Gasparovic, T. Wu, G. Wu, and X. H. Chen, *Phys. Rev. Lett.* **101**, 257003 (2008).
- ⁷⁹ M. Rotter, M. Tegel, D. Johrendt, I. Schellenberg, W. Hermes, and R. Pöttgen, *Phys. Rev. B* **78**, 020503(R) (2008).
- ⁸⁰ A. I. Goldman, D. N. Argyriou, B. Ouladdiaf, T. Chatterji, A. Kreyssig, S. Nandi, N. Ni, S. L. Bud'ko, P. C. Canfield, and R. J. McQueeney, *Phys. Rev. B* **78**, 100506(R) (2008).
- ⁸¹ J. Zhao, W. Ratcliff, II, J. W. Lynn, G. F. Chen, J. L. Luo, N. L. Wang, J. Hu, and P. Dai, *Phys. Rev. B* **78**, 140504(R) (2008).
- ⁸² D. J. Singh, *Phys. Rev. B* **78**, 094511 (2008).
- ⁸³ L. Zhang, A. Subedi, D. J. Singh, and M. H. Du, *Phys. Rev. B* **78**, 174520 (2008).
- ⁸⁴ D. Kasinathan, A. Ormeci, K. Koch, U. Burkhardt, W. Schnelle, A. Leithe-Jasper and H. Rosner, *New J. Phys.* **11**, 025023 (2009).
- ⁸⁵ Z. Li, J. S. Tse, and C. Q. Jin, *Phys. Rev. B* **80**, 092503 (2009).
- ⁸⁶ Y.-F. Li, B.-G. Liu, *Eur. Phys. J. B* **72**, 153 (2009).
- ⁸⁷ C.-Y. Moon, S. Y. Park, and H. J. Choi, *Phys. Rev. B* **78**, 212507 (2008).
- ⁸⁸ V. Vildosola, L. Pourovskii, R. Arita, S. Biermann, and A. Georges, *Phys. Rev. B* **78**, 064518 (2008).
- ⁸⁹ C.S. Liu, Y.L. Li, Y. Xu, X.L. Wang, and Z. Zeng, *Physica B* **404**, 3242 (2009).
- ⁹⁰ Y. Kamihara, H. Hiramatsu, M. Hirano, R. Kawamura, H. Yanagi, T. Kamiya, and H. Hosono, *J. Am. Chem. Soc.* **128**, 10012 (2006).
- ⁹¹ G. Baskaran, *J. Phys. Soc. Jpn.* **77**, 113713 (2008).
- ⁹² T. M. McQueen, M. Regulacio, A. J. Williams, Q. Huang, J. W. Lynn, Y. S. Hor, D. V. West, M. A. Green, R. J. Cava, *Phys. Rev. B* **78**, 024521 (2008).
- ⁹³ T. Nomura, S. W. Kim, Y. Kamihara, M. Hirano, P. V. Sushko, K. Kato, M. Takata, A. L. Shluger, H. Hosono, *Supercond. Sci. Technol.* **21**, 125028 (2008).
- ⁹⁴ G. F. Chen, Z. Li, D. Wu, G. Li, W. Z. Hu, J. Dong, P. Zheng, J. L. Luo, and N. L. Wang, *Phys. Rev. Lett.* **100**, 247002 (2008).
- ⁹⁵ J. Zhao, Q. Huang, C. de la Cruz, S. Li, J. W. Lynn, Y. Chen, M. A. Green, G. F. Chen, G. Li, Z. Li, J. L. Luo, N. L. Wang, P. Dai, *Nature Materials* **7**, 953 (2008).
- ⁹⁶ Z.-A. Ren, J. Yang, W. Lu, W. Yi, X.-L. Shen, Z.-C. Li, G.-C. Che, X.-L. Dong, L.-L. Sun, F. Zhou, and Z.-X. Zhao, *Europhys. Lett.* **82**, 57002 (2008).
- ⁹⁷ Y. Qiu, Wei Bao, Q. Huang, T. Yildirim, J. Simmons, J. W. Lynn, Y. C. Gasparovic, J. Li, M. Green, T. Wu, G. Wu, X. H. Chen, *Phys. Rev. Lett.* **101**, 257002 (2008).
- ⁹⁸ Z.-A. Ren, W. Lu, J. Yang, W. Yi, X.-L. Shen, Z.-C. Li, G.-C. Che, X.-L. Dong, L.-L. Sun, F. Zhou, and Z.-X. Zhao, *Chin. Phys. Lett.* **25**, 2215 (2008).
- ⁹⁹ A. Martinelli, M. Ferretti, P. Manfrinetti, A. Palenzona, M. Tropeano, M. R. Cimberle, C. Ferdeghini, R. Valle, M. Putti, A. S. Siri, *Supercond. Sci. Technol.* **21**, 095017 (2008).
- ¹⁰⁰ C.-H. Lee, A. Iyo, H. Eisaki, H. Kito, M. T. Fernandez-Diaz, T. Ito, K. Kihou, H. Matsuhata, M. Braden, and K. Yamada, *J. Phys. Soc. Jpn.* **77**, 083704 (2008).